#13

Toner Charge Instability

Robert J. Nash, Scott M. Silence and Richard N. Muller
Xerox Corporation, Webster, New York

Abstract

Toner triboelectric charge can be affected by a variety of intrinsic and extrinsic factors, and production and maintenance of a stable charge requires a balancing or minimization of many complex interactions. In this review, major stability factors are discussed and illustrated using actual experimental data coupled with a simple theoretical model. Throughout, the review promotes a holistic approach in order to reinforce the view that toner charge stability is not merely a toner issue.

1. Introduction

In conventional xerography, a latent electrostatic image is developed by triboelectrically-charged toner particles, and xerographic development (to a first order) is an inverse function of toner charge level.[1] From a toner viewpoint, then, triboelectric charge—its polarity, magnitude and stability—is a critical property, and the creation and maintenance of a functional charge value is a major materials design challenge.

Since toner charge is controlled by many intrinsic and extrinsic factors, absolute charge stability is effectively an unattainable goal, and a degree of charge variability must be assumed for any commercial xerographic product. Now, in practical xerographic copiers and printers, variations in toner charge can be compensated for via closed-loop control of other factors that affect development—for example, the electrostatic image potential—but such control schemes add the expense and complexity of image density sensors, electrostatic voltage sensors, environmental temperature/RH sensors, etc.[2-5] For robust simplicity, therefore, toner charge stability remains as an important ultimate design goal.

However, besides the problems outlined thus far, there are important additional toner design limits imposed by the functional requirements of the post-development subsystems, namely the transfer, cleaning and fusing subsystems. For example, toner adhesion and flow properties affect transfer and cleaning performance, and toner rheological and surface-chemical properties are important factors for efficient fusing. As a result, optimum performance in post-development is frequently achieved via incorporation of external and/or internal additives (e.g., flow aids, waxes, etc.) to the overall toner design, and unfortunately these additives may also affect toner charge level and stability.

Further, since toner triboelectric charge is generated through contacts with other charging surfaces—carrier beads for two-component xerography; donor roll surface and charging/metering blade or roll for single-component xerography—then the quality and stability of these non-toner surfaces must also be considered in any overall strategy for toner triboelectric charge stability.

Finally, all of the charging interactions listed thus far can also be affected by ambient environmental conditions, since triboelectric charging is especially sensitive to water vapor relative humidity.

All in all, then, triboelectric charge stability is a wide-ranging topic involving many potential complex interactions. To illustrate some of the major controlling factors for charge variability, the following discussion is based on "lessons" from experimental data, with a theoretical model for triboelectric charging being used as an overall conceptual framework.

2. Triboelectric Charging

2.1 Parametric Charging Equation

For a two-component xerographic developer, the toner charge-to-mass ratio, q/m, generated by mixing with carrier beads, can be related to the toner-to-carrier weight concentration, C, by:

$$q/m = [A_o / (C + C_o)] \cdot [1 - \exp\{-\gamma \cdot t\}] \qquad (1)$$

where A_o and C_o are characteristic parameters for any particular toner/carrier combination, t is the mixing time and γ• is the effective rate constant for the charging process. Now, all of the parameters in Eq. 1 contain contributions from the controlling physics and chemistry of triboelectric charging, and the impact of these contributions on charge stability will next be discussed sequentially in the following sections, in order of increasing complexity.

2.2 Charge Generation

The second term in Eq. 1 is a simple saturating exponential function, and is a functional form typically seen when a simple, additive-free toner is mixed with carrier beads. For this process, the effective rate constant[6] is:

$$\gamma = \gamma' (C + Co) \qquad (2)$$

where γ' is a direct function of the frequency of toner/carrier mixing contacts.

Thus, for any particular mixing time, a range of q/m values can be achieved simply via an appropriate choice of mixing intensity, and this charging/mixing response is commonly seen in actual mixing experiments.[7] From a charge stability viewpoint, of course, this mixing intensity effect is a potential source of variability in q/m, and should therefore be avoided. Clearly, an effective strategy would be to set the mixing intensity at a level high enough to

produce the limiting $A_o/(C + C_o)$ value of q/m after a short mixing time. However, as will be outlined in subsequent sections of this review, a high mixing intensity can itself create q/m variability through attendant "aging" processes—e.g., processes which affect the A_o parameter via permanent physico-chemical changes to the toner and/or carrier particles. Thus, even the seemingly simple toner/carrier mixing process requires careful process optimization in order to produce a stable q/m value. In practical terms, problems in this area typically occur when a single developer is used in a variety of process applications. For example, a developer which has been optimized for use in a high-volume xerographic machine may show sub-optimal q/m performance when used without modification in a low-volume product.

Mixing effects can also complicate comparisons between bench-test and actual machine operation, since bench-test mixers are generally used for the evaluation of small-scale experimental developers, and are therefore not likely to be functional surrogates of actual development housings. Indeed, for certain types of developers, the long-term, stable $A_o/(C + C_o)$ value of q/m varies significantly between mixer types, and can be repeatedly cycled between characteristic levels simply by periodic changes in the mode of mixing. Fig. 1 shows an example of this effect, and toner/carrier contact area differences created by mixing intensity differences,[6] and surface conductivity effects[7] have both been postulated as possible causes for this type of mixing effect—for both cases, the q/m level will be altered by a change in the magnitude of the A_o term in Eq. 1.

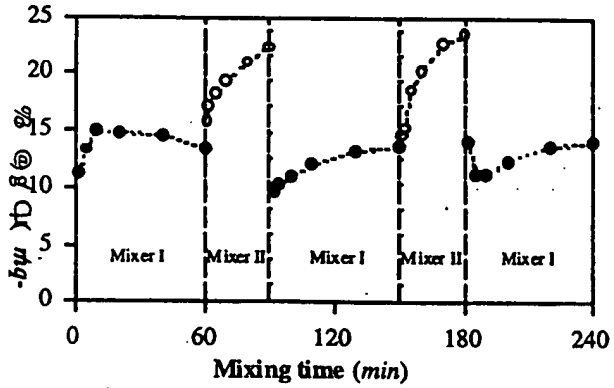

Figure 1. Effect of mixing conditions on q/m.

2.3 Toner Concentration and Size Effects

For an ideal, well-mixed developer, the long-term toner q/m value, as given by Eq. 1, will be:

$$q/m = A_o/(C + C_o) \qquad (3)$$

and this equation shows that even well-mixed developers can give a range of q/m values. For example, since parameters A_o and C_o are characteristic constants for any particular developer, then q/m is predicted to be an inverse function of the toner concentration, C. Thus, for any developer, there is no single "standard" q/m value, and a range of q/m values can be generated simply by an appropriate selection of the toner concentration.

Figure 2 shows a set of representative experimental q/m:C data (taken from a development housing operating over a range of toner concentration), and though both test developers are based on ferrite carriers, they clearly differ in their q/m:C responses. The difference in q/m magnitude at any single C value could be simply explained in terms of toner chemistry—the upper data are from a yellow, organic pigment-based toner while the lower are from a carbon black toner. The form of the q/m:C responses, however, reflect physical differences, specifically toner and carrier size—the black developer is based on an 8mm toner and a 150mm ferrite carrier, while the yellow developer is based on a 12.5μm toner and a 50μm ferrite carrier. These size differences affect the value of the C_o term in Eq. 1, since C_o is a direct function of toner size and is a direct inverse function of carrier size.[6] For the two developers shown in Figure 2, C_o = 1.4 wt% for the black developer and C_o = 7.5 wt% for the yellow developer. As a result, the q/m values for the latter developer have a greatly reduced sensitivity to variations in toner concentration, and from a q/m stability viewpoint this is a desirable result.

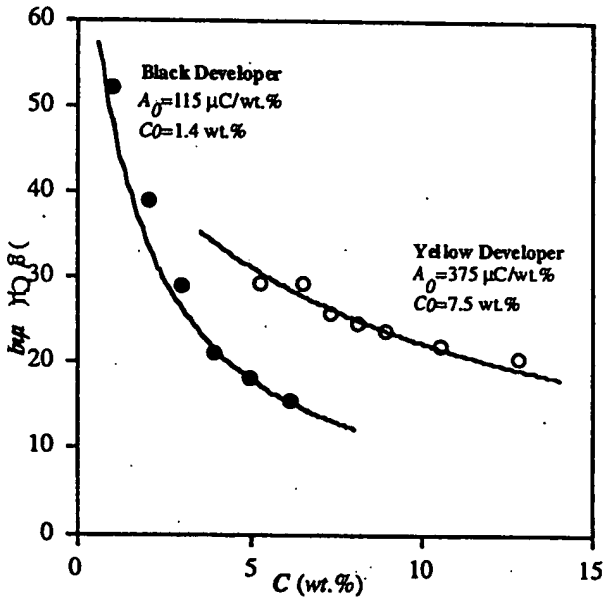

Figure 2. Effect of carrier size and toner size on q/m:C relationship. Experimental data from in-machine toner concentration scans.

Parametrically, the two developers in Figure 2 can be described by:

BLACK DEVELOPER: $q/m = 115 / (C + 1.4)$
YELLOW DEVELOPER: $q/m = 375/ (C + 7.5)$

and it might appear from the A_o values that the yellow developer has the highest intrinsic charging ability. However, the A_o parameter is a direct inverse function of carrier size,[6] and this carrier size dependence, coincidentally, largely accounts for the difference between the above developers. (In general, of course, the magnitude and polarity of A_o can be set at any desired value by an appropriate choice of toner and/or carrier chemistry).

Now, for the above example, the black and yellow developers differed in both toner and carrier size. For the

case of a single carrier size, changes in toner size will produce variability in q/m via variations in the C_o parameter, and since this latter term is a direct function of toner size, q/m will increase as toner size decreases. However, since the size effect operates via the C_o term,[6] the sensitivity of q/m to a toner size change will vary with toner concentration, C. The largest respons will be at low values of C, and this effect will be most evident in developers based on small carriers, as shown in Figure 3. In this figure, each q/m:C relationship is calculated for a fixed carrier size and fixed toner size, for two values of A_o as indicated. Clearly, an experimental determination of a q/m:toner size relationship will be of limited predictive value if taken at only a single toner concentration.

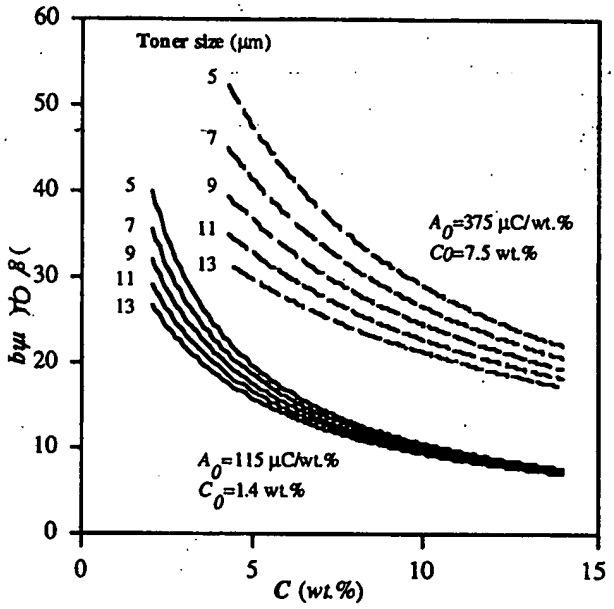

Figure 3. Calculated effect of toner size on q/m:C relationship for two sizes of ferrite carrier.

3. Developer Aging Effects

To highlight physico-chemical effects on triboelectric charging, it is convenient to rewrite the parametric q/m:C relationship for a fully-mixed developer as:

$$q/m = [A' (\phi_{toner} - \phi_{carrier})]/(C + C_o) \quad (4)$$

In Eq. (4) the ϕ_{toner} and $\phi_{carrier}$ terms represent, respectively, the toner and carrier charging tendencies (governed by their physico-chemical properties), and the A' term contains all of the purely physical terms (such as the electronic charge, the carrier mass, etc.).[6]

With this formalism, the $(\phi_{toner} - \phi_{carrier})$ difference term directly determines the polarity of q/m, and also directly affects the magnitude of q/m.

3.1 Carrier Coating Loss

Conceptually, the ϕ_{toner} and $\phi_{carrier}$ terms can be expressed in terms of surface area-weighted fractions of contributions from the various toner and carrier constituents.[6] For example, for a partially-coated carrier:

$$\phi_{carrier} = P_{coating} \cdot \mu_{coating} + P_{core} \cdot \mu_{core} \quad (5)$$

where the μ terms denote the respective constituent charging tendencies, and the P terms are the weighting factors. Since, by definition, the latter must sum to unity, Eq. 5 can be rewritten as:

$$\phi_{carrier} = P_{coating} \cdot (\mu_{coating} - \mu_{core}) + \mu_{core} \quad (6)$$

so that Eq. 4 becomes:

$$q/m = A' \cdot [\phi_{toner} - P_{coating} \cdot (\mu_{coating} - \mu_{core}) \quad (7)$$

For cases of developer aging involving wear-induced loss of carrier coating,[8] $P_{coating}$ will decrease as a function of "age", and (for cases where $\mu_{coating} \neq \mu_{core}$) this loss will produce an aging-time-dependent decrease or increase in q/m, with the direction of change being governed by the relative values of $\mu_{coating}$ and μ_{core}. For stability, therefore, it would appear that either $P_{coating}$ must remain fixed (i.e., no coating loss) or $\mu_{coating}$ must equal μ_{core}. However, since there can be other aging-induced mechanisms for q/m change, then there is always the possibility for stability achieved through a balancing of opposing effects. For example, for cases where $\mu_{core} > \mu_{coating}$, a degree of aged-induced coating loss could potentially provide an enhancement in q/m with "age" sufficient to counterbalance or even outweigh other q/m depressing aging mechanisms—see Figure 4, for example. Realistically, however, it is preferable to achieve stability via the elimination of aging factors.

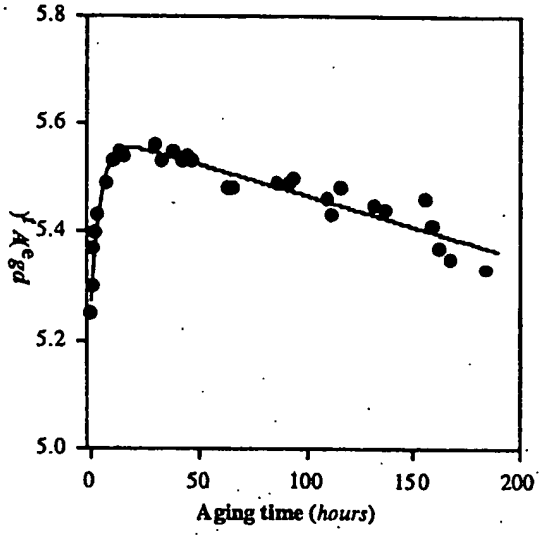

Figure 4. Initial age-induced increase in toner charging as a result of a partial loss of the carrier coating.

3.2 Toner Impaction

A common form of developer "aging" is that created by the gradual contamination of a carrier surface by permanently "welded" toner particles—the so-called toner impaction or scumming process. For this type of aging, the carrier charging term $\phi_{carrier}$, after a degree of toner impaction will be:

$$\phi_{carrier} = P_{carrier} \cdot \mu_{carrier} + (1 - P_{carrier}) \cdot \mu_{toner} \quad (8)$$

where $P_{carrier}$ is the fractional area of the carrier surface still left in its original uncontaminated state. (In this example, for simplicity, the coating and core contributions are combined into an single effective carrier term.)

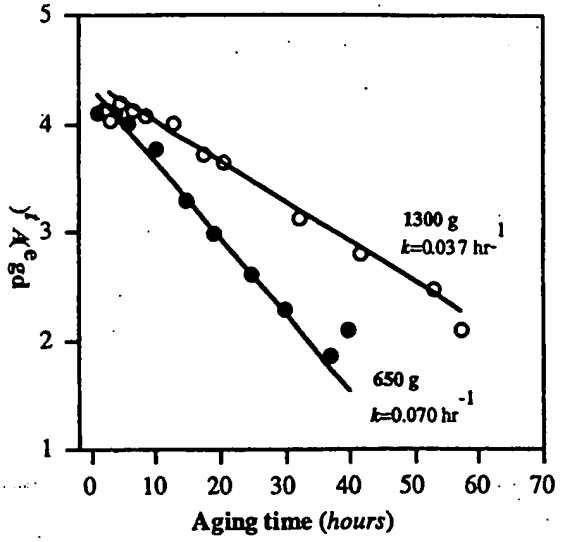

Figure 5a. Experimental triboelectric aging data from experiments made at two sump masses. (From Reference 9).

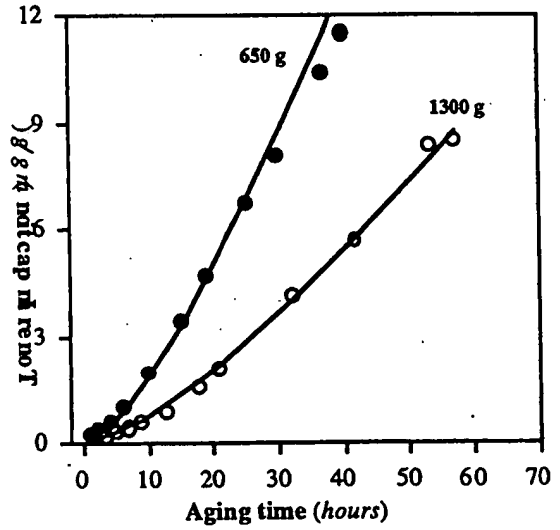

Figure 5b. Experimental toner impaction data from experiments made at two sump masses. (From Reference 9).

If the toner impaction process is a spatially-random process on the carrier surface, then at any aging time t,

$$P_{carrier} = exp\ \{-k \cdot t\} \quad (9)$$

and the effective rate constant k for the carrier "contamination" will be given by[9]:

$$k = (\nu \cdot \alpha \cdot a)/\Sigma \quad (10)$$

where ν is the frequency of carrier/toner collisions, α is a toner "sticking coefficient" (only a small proportion of collisions actually produce impacted toner), a is the carrier area obscured per successful impaction event, and Σ is the total carrier surface area.

Thus, at any aging time t

$$(\phi_{toner} - \phi_{carrier}) = [\mu_{toner} - (P_{carrier} \cdot \mu_{carrier}) + (1 - P_{carrier}) \cdot \mu_{toner})] \quad (11)$$

$$= [\mu_{toner} - \mu_{carrier}) \cdot exp\ \{-k \cdot t\} \quad (12)$$

and

$$q/m = [A' \cdot (\mu_{toner} - \mu_{carrier}) \cdot exp\ \{-k \cdot t\}]/(C + C_o) \quad (13)$$

$$= [A_o \cdot exp\ \{-k \cdot t\}]/(C + C_o) \quad (14)$$

From Eq. 14 it is clear that developer triboelectric aging can be monitored from the "aging" values of the A parameter calculated from q/m:C pairs taken throughout an aging experiment. Indeed, it is convenient to define an age-dependent value of A as A_t, i.e.:

$$A_t = q/m_t \cdot (C_t + C_o) \quad (15)$$

since this allows Eq. 14 to be simply rewritten as:

$$A_t = A_o \cdot exp\ \{-k \cdot t\}. \quad (16)$$

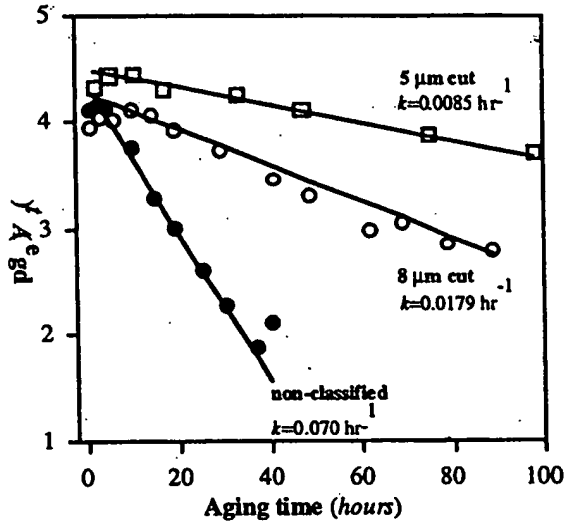

Figure 6a. Experimental triboelectric aging data from experiments made with three toner sizes (From Ref 9).

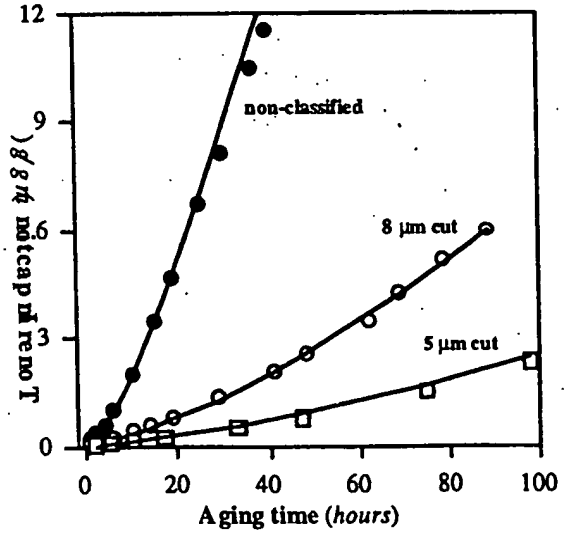

Figure 6b. Experimental triboelectric aging data from experiments made with three toner sizes (From Ref 9).

Now, from Eq. 16 it is clear that the effective rate constant k must be minimized to minimize age-induced changes in A_t (and thence in q/m_t) and effective strategies include maximizing the developer mass (thereby reducing the toner/carrier collision frequency), and elimination of highly-impactable toner particles from the feed toner. The former strategy can be readily demonstrated for developer housings having non-stagnant, quiescent sumps—see Figure 5, and the latter strategy can be achieved by selective sizeclassification of toner to reduce the concentration of "fines"—see Figure 6.

(The fines-driven impaction process can also be seen in no-throughput bench tests—in such tests, the toner impaction rate falls rapidly as toner fines are consumed, and the generation of a high level of impacted toner on the carrier beads requires periodic de-tone of "old" toner/re-tone with "fresh" toner).

Unfortunately, the "large-sump" life-extending strategy favored by developer materials designers is frequently counter to the "compact-housing" design goals of the development process engineers. One effective solution to these contrary requirements is the use of "replenisher" in place of dispensed toner.[10] "Replenisher" is a toner-rich mixture of toner and carrier particles, and the steady addition of "replenisher" to a working developer (coupled with an equivalent draining-off of partially-used developer) allows an otherwise aging developer to stabilize at a functional equilibrium value. For example, for a developer which would normally age according to Eq. 16, a "replenisher" addition process having an effective rate constant r (expressed as grams of carrier added per unit time per unit total carrier mass in the sump) will cause the developer to age according to[10]:

$$A_t = A_o - [A_o \cdot (1 - (exp\ \{-(k + r) \cdot t\}))/(1 + r/k)], \quad (17)$$

and after extended operation, the developer will therefore stabilize at:

$$A_\infty = A_o \cdot [1 - \{k/(k + r)\}]. \quad (18)$$

3.3 CCA-Transfer

For a toner which contains a charge control agent (CCA), the component contributions can be segregated according to:

$$\phi_{toner} = P_{resin} \cdot \mu_{resin} + P_{colorant} \cdot \mu_{colorant} + P_{CCA} \cdot \mu_{CCA} \quad (19)$$

with

$$P_{resin} + P_{colorant} + P_{CCA} = 1. \quad (20)$$

Now, while CCA's can strongly impart desired charging characteristics to toner particles, they must also (by analogy) be viewed as potential "poisons" with respect to the charging characteristics of carrier particles. Therefore, age-induced transfer of CCA from toner to carrier must be considered as a potential source of q/m instability. Experimentally, CCA-transfer has been shown to cause a significant depression of developer charging capability,[11-15] and toners with high levels of CCA can cause an ultra-high rate of aging.[11]

During normal imaging conditions with a constant toner throughput, CCA transfer to carrier particles can occur without an appreciable change in the CCA content of the toner particles, and under such conditions the CCA-induced developer aging will follow:

$$A_t = (A_o - A_\infty) \cdot exp\ \{-\delta \cdot t\} + A_\infty, \quad (21)$$

where δ is the effective rate constant for the CCA-transfer process, and :

$$A_o = A_o \cdot [1 - \{P_{CCA} \cdot (\mu_{CCA} - \mu_{carrier})/(\mu_{toner} - \mu_{carrier})\}] \quad (22)$$

where P_{CCA} is the long-term fractional coverage of CCA on the carrier.

In general, however, CCA-transfer is more complex than the simple process just outlined. For example, during initial developer blending, toner and carrier particles are normally mixed without toner throughput, and blending may therefore affect the CCA level of both toner and carrier.[11,15] For such a case, the subsequent gradual replacement of blend toner by feed toner during xerographic imaging can then produce an initial age-induced increase in developer triboelectric charging capability, and the overall simultaneous occurrence of charge-enhancing and charge-depressing processes can produce a complex aging profile. Frequently, such aging can be parametrically described by:

$$A_t = A_1 \cdot exp\ \{-r_1 \cdot t\} - A_2 \cdot exp\ \{-r_2 \cdot t\} + A_3 \quad (23)$$

where A_1, A_2 and A_3 are constants and r_1 and r_2 are the effective rate constants for the degradation and enhancement processes, respectively.

However, an in-depth study of the aging effects seen with a typical CCA-containing toner[15] indicates that the CCA transfer process to the carrier is not permanent, but is in fact reversible. Thus, the parameters A_1, A_2, A_3, r_1 and r_2 in Eq. 23 are not true constants, since the point of toner/carrier CCA equilibration can be altered by external factors. For example, aging at a low toner concentration favors CCA transfer to carrier particles (presumably as a result of increased particle-particle friction) and this creates a high level of triboelectric aging—see Figure 7.

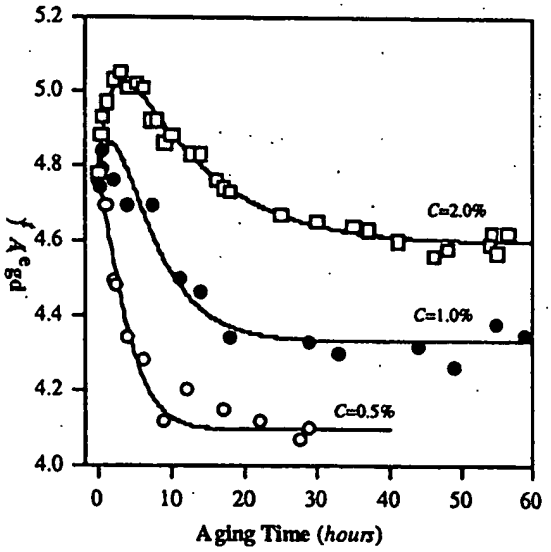

Figure 7. Triboelectric aging data from tests made at three toner concentrations with a single CCA-toner. The lines are for a common fit to the entire data set. (From Ref 15).

Now, while CCA transfer can create complex aging behavior, it does offer an important advantage for stability, namely the zero aging rate produced by the long-term toner/carrier CCA equilibration. If this latter balance point occurs at a reasonable value of A_r, then a developer based on a CCA-toner would appear to meet the design goals of a truly robust developer. However, even for a CCA-developer, stability can be affected by several other intrinsic and extrinsic factors, and these additional effects will be outlined in the following sections.

4. External Additive Effects

4.1 Particulate Additives

While particulate external additives can enhance toner properties such as adhesion, cohesion, flow etc., they can also affect *q/m* level and can adversely affect *q/m* stability.[16,17] These effects can be readily modeled using the patch-wise view of charge generation outlined in the previous sections of this survey. For example, with this view, a toner treated with an particulate external additive can be described by:

$$\phi_{toner} = P_{toner} \cdot \mu_{toner} + P_{extl.add.} \cdot \mu_{extl.add.} \quad (24)$$

$$= P_{extl.add.} \cdot (\mu_{extl.\ add.} - \mu_{toner}) + \mu_{toner} \quad (25)$$

i.e., the contributions from the constituents of the base toner (e.g., resin, colorant, CCA etc.) are all combined into an single μ_{toner} term, and $P_{extl.\ add.} + P_{toner} = 1$.

For short-term developer mixing, a particulate external additive toner will generate *q/m* values according to:

$$q/m = [A' \cdot (\phi_{toner} - \phi_{carrier}) \cdot (1 - exp\ \{-\gamma \cdot t\})]/(C + C_o) \quad (26)$$

$$= [A' \cdot (P_{extl\ add.} \cdot (\mu_{extl.\ add.} - \mu_{toner}) + \mu_{toner} - \mu_{carrier}) \cdot (1 - exp\ \{-\gamma \cdot t\})]/(C + C_o) \quad (27)$$

and extended mixing should generate a stable toner charge given by:

$$q/m = [A' (P_{extl.\ add.} \cdot (\mu_{extl.\ add.} - \mu_{toner}) + \mu_{toner} - \mu_{carrier})]/(C + C_o) \quad (28)$$

This latter equation can be rearranged to give:

$$q/m = [A' \cdot (P_{extl.\ add.} \cdot (\mu_{extl.\ add.} - \mu_{carrier}) + (1 - P_{extl.\ add.}) \cdot (\mu_{toner} - \mu_{carrier})]/(C + C_o) \quad (29)$$

a form which highlights the silica/carrier and toner/carrier charging contributions.

For a two-dimensional surface distribution of external particles, the surface percent coverage, θ, will be a direct linear function of additive concentration by weight percent, and a direct inverse function of additive size.[18] Thus, for any single particulate external additive, the $P_{extl.\ add.}$ term should be directly proportional to the additive weight percent concentration up to a monolayer coverage. Therefore, from Eq. 28, it can be seen that increasing levels of a particulate external additive should create a linear increase (or linear decrease) in toner *q/m*, with the sign and magnitude of the *q/m* change being driven by the value of $\theta \cdot (\mu_{extl.\ add.} - \mu_{toner})$.

Figure 8 shows a typical *q/m*:mixing time experimental result for addition of a 8nm, "negative", hydrophobic fumed silica additive to a toner in a negative polarity developer. For this data set, at any fixed mixing time, the change in toner *q/m* value from the additive-free case is linear in silica surface concentration, as predicted by Eq. 27. Experimentally, for any particular toner/carrier pair, this seems to be a general result for "negative" fumed silica external additives, independent of silica particle size and/or surface treatment—the key controlling factor appears to be the area concentration, θ, of silica on the toner surface.

From Eq.27 the *q/m*:silica surface coverage response is predicted to be:

$$\partial(q/m)/\partial\theta = [A' \cdot (\mu_{extl.\ add.} - \mu_{toner})]/(C + C_o), \quad (30)$$

so that a common silica response implies a common value of μ_{silica}.

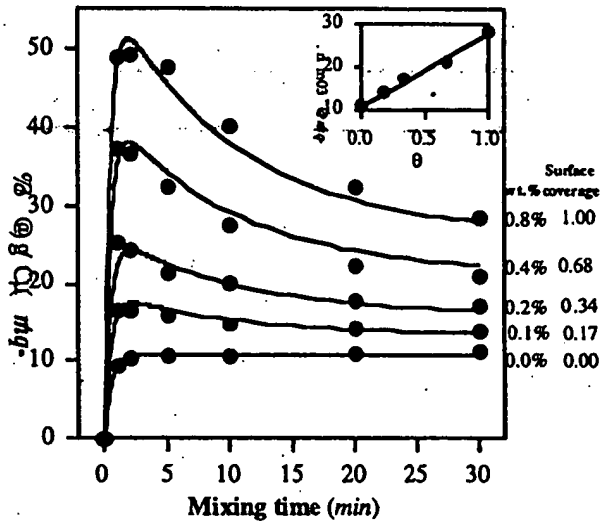

Figure 8. Effect of 8nm, particulate "negative" SiO_2 on the q/m of a negative polarity developer. (Lines are for a common fit to the entire data set-see text).

Now, the additive effect shown in Figure 8 is clearly more complex than that predicted by Eq. 27—in particular, the experimental data show a long-term degradation of *q/m*, and parametrically the data follow:

$$q/m = (q/m_1 - q/m_2) \cdot exp\ (-k \cdot t) - q/m_1 \cdot exp\ (-\gamma \cdot t) + q/m_2, \quad (31)$$

a form which describes *q/m* charging (from an initial zero level) in terms of charge generation towards level q/m_1 coupled with a simultaneous process which drives the system to an eventual long-term level, q/m_2.

Mechanistically, it appears that the silica-driven *q/m*-enhancement effect seen at short mixing times in Figure 8 is systematically reduced by extended mixing, and one possible explanation is that continued developer mixing "buries" the silica particles into the toner sub-surface. With this view (as with other "loss" pathways) the $P_{extl.\ add.}$ term will be time-dependent, and the form of the experimental data suggests a dependency which follows:

$$P_{extl.\ add.} = \theta \cdot [1 - F \cdot (1 - exp\ \{-k \cdot t\})] \quad (32)$$

where θ is the time-zero additive surface concentration, and *F* is the fraction of additive "lost" after extended mixing.

Substitution of this time-dependent expression for $P_{extl.\ add.}$ into Eq. 27 yields:

$$q/m = [A' \cdot ((\theta \cdot (1 - F \cdot (1 - exp\{-k \cdot t\}))) \cdot (\mu_{extl.\ add.} - \mu_{toner}) + \mu_{toner} - \mu_{carrier}) \cdot (1 - exp\{-\gamma \cdot t\})]/(C + C_o) \quad (33)$$

or,

$$q/m = [A' \cdot (\theta \cdot (1 - F \cdot (1 - exp\{-k \cdot t\}))) \cdot (\mu_{extl.\ add.} - \mu_{carrier}) \cdot (1 - exp\{-\gamma \cdot t\})]/(C + C_o) + [((1 - \theta) + (\theta \cdot F) \cdot (1 - exp\{-k \cdot t\})) \cdot (\mu_{toner} - \mu_{carrier})] \cdot (1 - exp\{-\gamma \cdot t\})]/(C + C_o) \quad (34)$$

and these equations are functionally equivalent to the parametric Eq. 31.

Unfortunately, parameters such as $\mu_{extl.\ add.}$, μ_{toner} and $\mu_{carrier}$ cannot be directly measured, and actual triboelectric charge measurements can only yield values for combinations of parameters (e.g., the long-term *q/m* value for the base additive-free toner plus carrier will be $[A' \cdot (\mu_{toner} - \mu_{carrier})]/(C + C_o)$). However, it is instructive too estimate a value for A', deconvolute the experimental data according to Eq. 34 and thence obtain values for $(\mu_{extl.\ add.} - \mu_{carrier})$, $(\mu_{toner} - \mu_{carrier})$, F etc. For the developer used in Figure 8, reasonable values for carrier size, mass, charge tunneling distance, etc. give $A' = 70\mu C \cdot g^{-1} \cdot eV^{-1}$, with terms such as $(\mu_{extl.\ add.} - \mu_{carrier})$ expressed in eV.

For the entire data shown in Figure 8, a common fit can be obtained with:

Assumed values:
$A' = 70\ \mu C \cdot g^{-1}$, $\theta = 1.69 \cdot$ (silica wt%)

Deduced values:
$F = 0.67$, $k = 0.1\ min^{-1}$, $\gamma = 2.0\ min^{-1}$,

$(\mu_{toner} - \mu_{carrier}) = -0.56$ eV,
$(\mu_{extl.\ add.} - \mu_{toner}) = -2.53$ eV,
$(\mu_{extl\ add.} - \mu_{carrier}) = -3.09$ eV,

and the fits obtained with these values are shown in Figure 8 (lines).

Thus, the analysis shows that for each level of silica there is a longterm 67% loss of toner surface additive, and the single value of *k* indicates that the loss mechanism has a common mode for all of the silica levels. ("Burial" of fine silica additives is a commonly observed effect, and strategies proposed to minimize the loss include the use of a "run-time" toner with an additive level higher than the blend toner,[19] the use of a dual vigorous/gentle blend process,[20] and the use of friable silica/polymer composites as a run-time source of silica.[21] The use of "large" additives—both SiO_2 and TiO_2—has also been proposed as a means to minimize additive "burial" effects [18,19]).

For the example shown in Figure 8, the fumed silica additive can clearly provide a large increase in negative toner charge, but the mixing-induced eventual decline in charge enhancement introduces a new source of instability. However, silica-loss decreases in *q/m* should be less severe in actual xerographic applications since development involves a continual throughput of fresh toner, whereas in a bench-test mixing experiment a single aliquot of toner is used for the entire test.

The bench tests results, however, do suggest that extended zero-throughput mixing in an actual machine may depress *q/m*, and this is counter to the commonsense engineering view that vigorous mixing will ensure a maximum toner charge.

To complete this discussion of silica effects, Figure 9 is a clear demonstration that external additive effects apply equally to negative and positive developers. In this example, the toner contains a positive polarity CCA and generates positive *q/m* values.

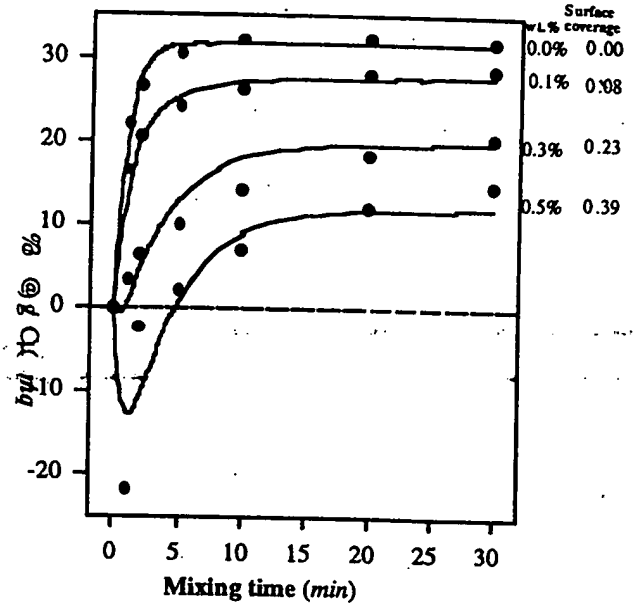

Figure 9. Effect of 16nm, particulate "negative" SiO_2 on the q/m of a positive polarity developer. (Lines are for a common fit to the entire data set—see text.)

As shown, addition of a 16 nm "negative" fumed silica as an external additive to this toner produces a systematic decrease in the positive *q/m* values, and a high level of external additive actually reverses the polarity of the toner at short mixing times. Once again, however, there is a long-term "loss" of silica additive, and for the pairing of a "positive" toner with a "negative" silica, this "loss" allows *q/m* to increase back towards the silica-free base toner value. This "reverse additive" behavior can still be described in terms of the mechanisms embodied in Eq. 34, and deconvolution of the "positive" toner data yields:

Assumed values:
$A' = 55\ \mu C \cdot g^{-1}$, $\theta = 0.78$ (silica wt%)

Deduced values:
$F = 0.67$, $k = 0.28\ min^{-1}$, $\gamma = 1.04\ min^{-1}$,

$(\mu_{toner} - \mu_{carrier}) = +2.30$ eV,
$(\mu_{extl.\ add.} - \mu_{toner}) = -8.66$ eV,
$(\mu_{extl\ add.} - \mu_{carrier}) = -6.36$ eV,

and the fits obtained with these values are shown in Figure 9 (lines).

Mechanistically, of course, the above external additive-induced depression in charge is a general result—the condition for charge depression (for $\theta > 0$) is simply $\mu_{extl.\ add.} > \mu_{toner}$ for negative developers, and $\mu_{extl.\ add.} < \mu_{toner}$ for positive developers.

Now many toner designs are actually based on multiple external additives, e.g., SiO_2/TiO_2,[19,22] SiO_2/Al_2O_3,[23] SiO_2/

Kynar,[24] SiO_2/zinc stearate,[25,26] SiO_2/zinc stearate/TiO_2,[27] etc. and the above analysis can be extended accordingly. For additives 1, 2 and 3, the general expression for *q/m* (assuming no additive-additive interactions) will be:

$$q/m = [A' \cdot (P_1 \cdot \mu_1 + P_2 \cdot \mu_2 + P_3 \cdot \mu_2 + P_{toner} \cdot \mu_{toner} - \mu_{carrier}) \cdot (1 - exp\ \{-\gamma \cdot t\})]/(C + C_o) \quad (35)$$

or

$$q/m = [A' \cdot (P_1 \cdot (\mu_1 - \mu_{carrier}) + P_2 \cdot (\mu_2 - \mu_{carrier}) + P_3 \cdot (\mu_3 - \mu_{carrier}) + (1 - P_1 - P_2 - P_3) \cdot (\mu_{toner} - \mu_{carrier})) \cdot (1 - exp\ \{-\gamma \cdot t\})]/(C + C_o) \quad (36)$$

(a form which highlights the individual toner component interactions with the carrier), or:

$$q/m = [A' \cdot ((\mu_{toner} - \mu_{carrier}) - P_1 \cdot (\mu_{toner} - \mu_1) - P_2 \cdot (\mu_{toner} - \mu_2) - P_3 \cdot (\mu_{toner} - \mu_3)) \cdot (1 - exp\ \{-\gamma \cdot t\})]/(C + C_o) \quad (37)$$

a form which highlights the weighted effects of each additive on the toner charging properties).

Since the various P terms in the above equations will likely have individual non-linear mixing-time dependencies, the overall effect of multiple additives on *q/m* can be quite complex. However, the relative stability of commercial toner designs indicates that variability can be minimized through a judicious balancing of additive concentrations.

Finally, for particulate external additives, the continued flow of fresh toner through a working developer will reduce mixing-induced changes in the concentration of toner external additives—in effect, toner-throughput can be viewed as the toner analogue of the carrier "replenisher" concept previously noted in the "aging" section of this review. However, for multiple additives, changes in toner throughput rate may create *q/m* variability, and stressful conditions such as zero-throughput (e.g., housing operation during machine start-up or cycle-out) should be minimized.

4.2 Filming Additives

Film-forming additives such as metal fatty acid salts are commonly used to promote effective blade cleaning[28] or to enhance developer conductivity,[25,29] and in principle the effect of such additives on *q/m* stability can be modeled as outlined for particulate additives. There is, however, an important difference between the two classes of additives—film-forming additives can affect the triboelectric properties of both toner and carrier particles, since such additives can be readily transferred between contacting surfaces. Thus, in an initial toner/additive blending step, the toner surface may become increasingly filmed with additive, and during the subsequent developer blending step (where carrier particles are mixed with a set concentration of toner), the carrier surface may receive a degree of additive filming. Indeed, for certain applications, it may be preferable to treat the carrier particles with a filming additive in a separate blending step.[30,31]

To further complicate matters, these filming processes may continue even during bench test evaluations of developers or during machine use, and this can produce complex *q/m*:mixing time responses. Figure 10 shows a set of representative *q/m*:mixing time data for a toner with several levels of a metal stearate external additive. For this test developer, the base toner/carrier combination gives a classic, stable *q/m*:mixing time response, and low levels of filming additive give a small enhancement in *q/m*. For high levels of filming additive, however, *q/m is* slightly enhanced at short mixing times, but is sharply depressed after extended mixing.

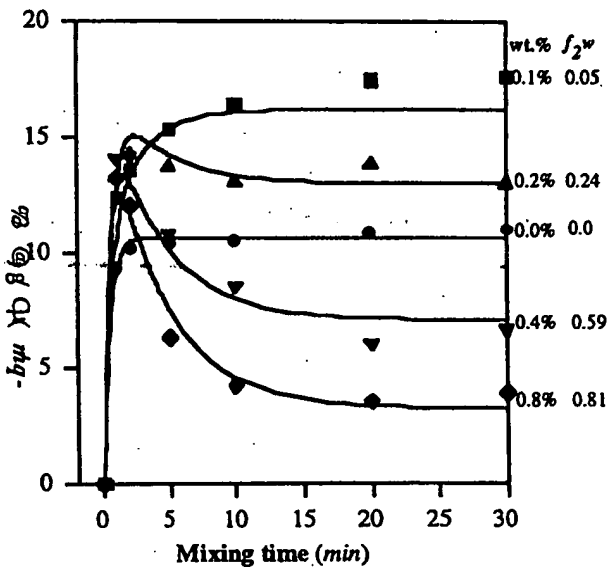

Figure 10. Effect of film-forming, metal stearate level on the q/m of a negative polarity developer. (Lines are for a common fit to the entire data set—see text).

The above effects will now be described in terms of additive-induced changes to both ϕ_{toner} and $\phi_{carrier}$. To separate toner and carrier effects, the additive film on the toner will be denoted by the subscript *tf*, and that on the carrier by *cf*.

Thus:

$$\phi_{toner} = P_{toner} \cdot \mu_{toner} + P_{tf} \cdot \mu_{film} \quad (38)$$

$$= (1 - P_{tf}) \cdot \mu_{toner} + P_{tf} \cdot \mu_{film} \quad (39)$$

and, similarly,

$$\phi_{carrier} = (1 - P_{cf}) \cdot \mu_{carrier} + P_{cf} \cdot \mu_{film}. \quad (40)$$

To mimic a rapid and complete filming of the toner particles, let

$$P_{tf} = 1 - exp\ \{-f_1 \cdot w \cdot t\} \quad (41)$$

where *w* is the wt% concentration of filming additive in the toner blend, and f_1 is a scaling factor.

To mimic a slower, partial filming of the carrier particles, let

$$P_{cf} = (f_2 \cdot w) \cdot (1 - exp\ \{-k \cdot t\}) \quad (42)$$

where f_2 is a scaling factor.

Then, as before

$$q/m = [A' \cdot ((\phi_{toner} - \phi_{carrier}) \cdot (1 - exp\ \{-\gamma \cdot t\}))]/(C + C_o)$$

$$= [A' \cdot ((1 - exp\ \{-f_1 \cdot w \cdot t\}) \cdot (\mu_{film} - \mu_{carrier})$$

$$+ (f_2 \cdot w) \cdot (1 - exp\ \{-k \cdot t\}) \cdot (\mu_{toner} - \mu_{film})$$

$$+ (exp\{-f_1 \cdot w \cdot t\} - (f_2 \cdot w) \cdot (1 - exp\{-k \cdot t\}))$$

$$\cdot (\mu_{toner} - \mu_{carrier})) \cdot (1 - exp\{-\gamma \cdot t\})]/(C + C_o). \quad (43)$$

For the fit shown in Figure 10, the following values were used:

Assumed value:
$A' = 70\ \mu C \cdot g^{-1}$

Deduced values:
$k = 0.24\ min^{-1}$, $\gamma = 2.0\ min^{-1}$,

$$f_1 \cdot w = 7\ min^{-1} \cdot (wt\%\ film\ add)$$
$$(\mu_{toner} - \mu_{carrier}) = -0.56\ eV,$$
$$(\mu_{toner} - \mu_{film}) = +0.33\ eV$$

One final note with respect to filming additives: the low *q/m* value generated after long-term mixing at a high additive concentration reflects a high level of additive film on the carrier and on the toner particles—both types of particles essentially present a similar filmed surface and therefore look almost identical from a triboelectric charging viewpoint. In practical developer designs, however, filming additives are typically paired with particulate additives,[26,27,30,31] thus allowing usable levels of toner charge to be generated. Though actual data from such mixed additive systems may be described in terms of simple parametric expressions, an in-depth analysis will be necessarily complex because of the possibility of simultaneous interactions of multiple additives with both toner and carrier particles.

4. Humidity Effects

The effect of ambient conditions on triboelectric charging is particularly troublesome since the effect can add sporadic, transitory or periodic contributions to all of the instability factors discussed thus far. Since xerographic machines must function over a wide range of ambient conditions (e.g., from 60°F/20% RH to 80°F/80% RH), many RH stability strategies have been developed. From a materials viewpoint, strategies include hydrophobic treatments for external additives,[19,32-35] or other developer components,[30,36,37] and the elimination of hydrophilic contaminants.[38,39] From a hardware viewpoint, an RH sensor is being increasingly used in process control modules.[2,4,5]

Mechanistically, the effect of RH is probably the most controversial aspect of triboelectric charging, and in part this reflects the experimental difficulties associated with RH/charging studies.[40] As an example of the potential problems posed by experimental data, consider the extremely unstable results shown in Figure 11. For this data set, the carrier is a heterogeneous carrier normally used with positive toners (oxidized steel core, partially-coated with a fluoropolymer), and the negative toner is based on a combination of two particulate external additives plus a filming additive—all in all a developer recipe likely to accentuate multiple competing interactions. While this developer gives a single value of *q/m* after 7 minutes of mixing at 60/20 or 80/80 (i.e., appears RH-stable at that particular mixing time), the total response is most unstable. Clearly, the RH-responses of the various developer components all differ with respect to magnitude and rate of change, thus producing the observed complex overall developer response. Conceptually, changes in charge magnitude reflect RH effects on the basic charging mechanisms, and mixing time-dependent changes reflect RH effects on the additive transfer/burial mechanisms. Though the RH data in Figure 11 are describable by simple parametric equations, an unequivocal mechanistic description cannot be derived because of multiple and simultaneous contributions to the measured *q/m* values. Indeed, the major qualitative lessons from Figure 11 are that the RH response of all components of a developer must be considered, and that RH effects can involve both the charging level and charging/mixing profile.

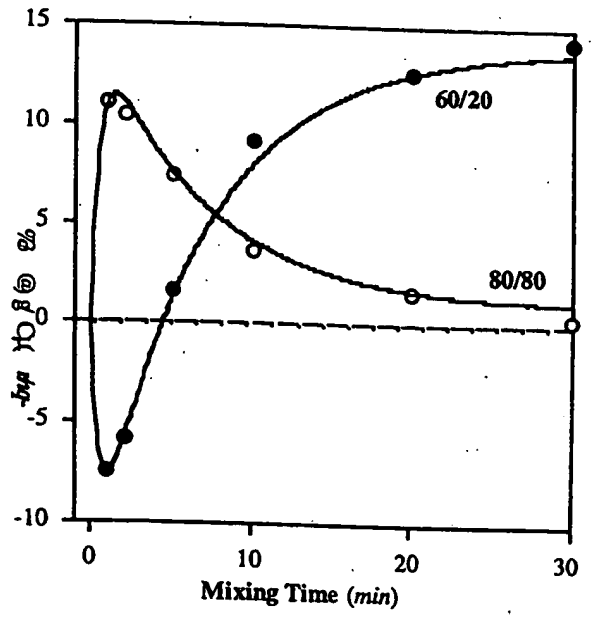

Figure 11. q/m:mixing time at 60/60 and 80/80 for a complex developer.

Now, the above concepts can be most easily demonstrated using simple model systems, and Figure 12 shows experimental data for a developer free of external additives. This particular developer, especially for medium mixing times, gives a *q/m* value which is unaffected by RH. However, since this *q/m* value is somewhat low, it would appear reasonable to add a 8nm hydrophobic fumed silica as an external additive to the toner in order to increase *q/m* and Figure 13 shows the result of such an addition. As expected, there is a significant increase in *q/m*—unfortunately, the addition of the hydrophobic silica also introduces a large sensitivity to RH, and a large mixing-induced instability. Significantly, a similar enhancement and response to RH is also seen when the added silica is changed to an 8nm hydrophilic form—see Figure 14.

Now, the concepts previously outlined in the external additives discussion can be used as a self-consistent framework for the above RH data. As before, mixing-driven changes in *q/m* will be modeled via time-dependent P factors, and the RH response of the magnitude and polarity of *q/m* will be assumed to be driven by the RH-sensitivity of the component m factors. For example, as discussed earlier, the simple toner/ carrier data in Figure 11 can be described by:

$$q/m = [A' \cdot (\mu_{toner} - \mu_{carrier}) \cdot (1 - exp\ (-\gamma \cdot t))]/(C + C_o) \quad (44)$$

and from the experimental data at both RH conditions, the *q/m* at 3wt% toner concentration (for a C_o value of 1) can be described by:

$$q/m = [70 \cdot (-0.61) \cdot (1 - exp\ \{-1.0 \cdot t\})]/(3 + 1). \quad (45)$$

For the experimental data from the toner combined with a hydrophobic silica (shown in Figure 13), the general conceptual equation (as detailed in the earlier discussion of particulate external additives) is:

$$q/m = [A' \cdot (\theta \cdot (1 - F \cdot (1 - exp\ \{-k \cdot t\})) \cdot (\mu_{silica} - \mu_{toner}) + \mu_{toner} - \mu_{carrier}) \cdot (1 - exp\ \{-\gamma \cdot t\})]/(C + C_o) \quad (46)$$

and for the 60/20 data shown in Figure 13, an analysis with Eq. 46 as the fitting function (with $A' = 70$) yields a predicted *q/m* value at a 3% toner concentration of:

$$q/m = 70 \cdot (1.0 \cdot (1 - 0.5 \cdot (1 - exp\ \{-0.10 \cdot t\})) \cdot (-2.54) - 0.61) \cdot (1 - exp\ \{-2 \cdot t\})]/(3 + 1) \quad (47)$$

and for the 80/80 data the predicted *q/m* value is:

$$q/m = 70 \cdot (1.0 \cdot (1 - 0.5 \cdot (1 - exp\ \{-0.20 \cdot t\})) \cdot (-0.71) - 0.61) \cdot (1 - exp\ \{-5 \cdot t\})]/(3 + 1) \quad (48)$$

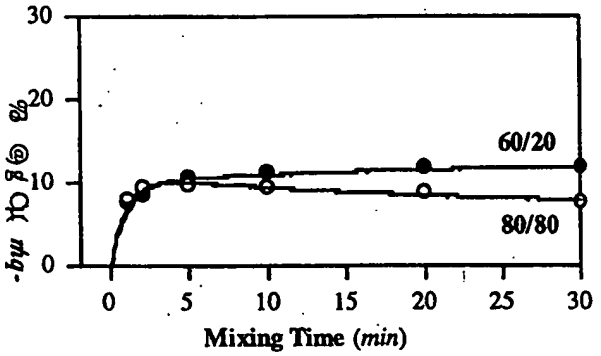

Figure 12. q/m:mixing time for an additive-free developer at 60/20 and 80/80.

Overall, then, four difference values can be deduced from the experimental data taken at two RH conditions. For the hydrophobic silica case:

$$(\mu_{toner} - \mu_{carrier})_{60/20} = -0.61 \text{ eV},$$
$$(\mu_{toner} - \mu_{carrier})_{80/80} = -0.61 \text{ eV},$$
$$(\mu_{silica} - \mu_{toner})_{60/20} = -2.54 \text{ eV},$$
$$(\mu_{silica} - \mu_{toner})_{80/80} = -0.71 \text{ eV},$$

while for the hydrophilic silica case shown in Figure 14 (same base toner), the analysis gives:

$$(\mu_{silica} - \mu_{toner})_{60/20} = -2.25 \text{ eV},$$
$$(\mu_{silica} - \mu_{toner})_{80/80} = +0.04 \text{ eV}.$$

With the above assumptions, the analysis indicates that the apparent absence, in Figure 14, of any long-term decay in the *q/m*:mixing profile of the 80/80 data is a result of the near zero value for the $(\mu_{silica} - \mu_{toner})$ term—if both toner and silica charge similarly, then the measured *q/m* value will be only weakly affected by any changes in silica content.

By themselves, the deduced difference values do not provide unique solutions, but they do allow an assessment of various extreme hypothesized mechanisms.

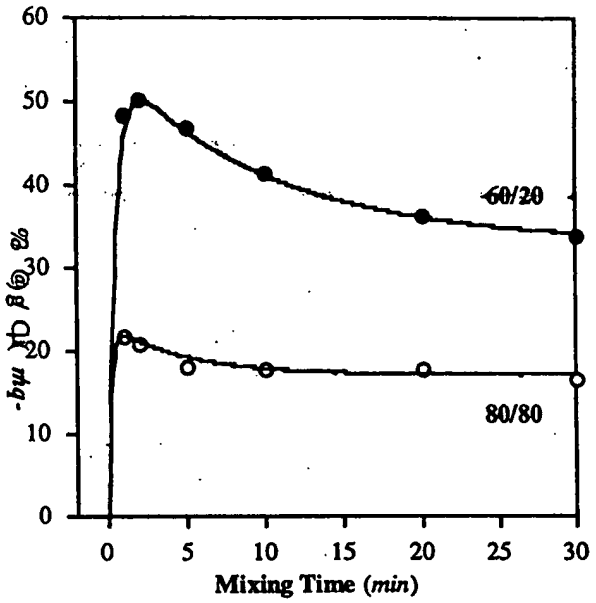

Figure 13. q/m:mixing time at 60/20 and 80/80 for a negative polarity developer, with 0.6 wt% of an 8nm, particulate, hydrophobic SiO_2 as an external toner additive.

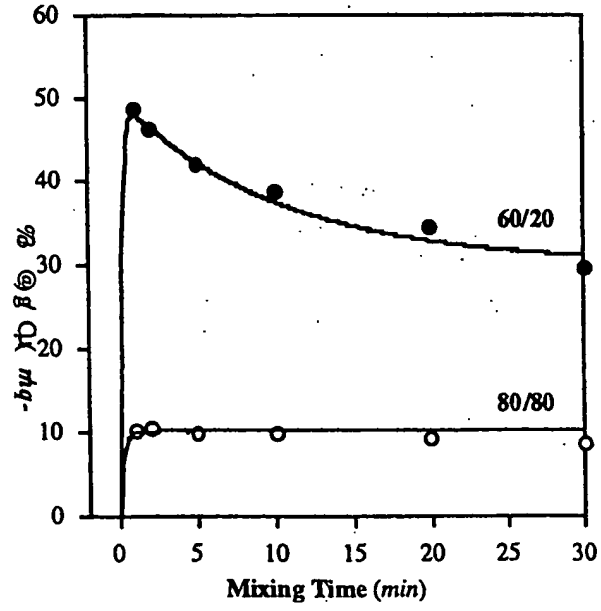

Figure 14. q/m mixing time at 60/20 and 80/80 for a negative polarity developer, with 0.6 wt% of an 8nm, particulate, hydrophilic SiO_2 as an external toner additive.

For example:

Assumption (a): the **toner** is totally RH-stable.

For this case, the carrier must also be RH-stable, since the difference term ($\mu_{toner} - \mu_{carrier}$) is identical at both RH conditions. Also, μ_{silica} must be an increasing function of RH, as indicated by the RH response of the difference term ($\mu_{silica} - \mu_{toner}$).

Assumption (b): the **silica** is totally RH-stable.

For this case, μ_{toner} must be a decreasing function of RH, and $\mu_{carrier}$ must respond identically, in order to keep a constant value of ($\mu_{toner} - \mu_{carrier}$) across the RH range.

Between the two extreme cases just described, there is, of course, a continuum of solutions based on cases where μ_{toner}, $\mu_{carrier}$ and μ_{silica} are all hypothesized to respond to RH, and the only certainty from the experimental data is:

$$\Delta\mu_{toner}/\Delta RH = \Delta\mu_{carrier}/\Delta RH.$$

Mechanistically, hydrophobic and hydrophilic silicas may represent the extremes in RH-stability strategies—for the former, stability may reflect a limited silica/water vapor interaction over the entire RH range, while for a hydrophilic silica a strong silica/water vapor interaction at all RH's may likewise confer stability. For both cases, stability merely indicates a constancy in $\Delta\mu_{silica}/\Delta RH$, without regard to the absolute value of μ_{silica}. Of course, in practical systems, there may be other properties (e.g., toner flow) that mandate the use of hydrophobic silicas, but from an RH-stability viewpoint, both hydrophobic and hydrophilic silicas may or may not confer RH-stability to an overall developer design.

Despite all of the above difficulties (which, of course, are characteristic of all difference-driven phenomena) several important conclusions can be deduced. For example, the general analysis illustrates that contributions from all developer components (i.e., toner, carrier and external additives) affect the RH-response of a developer. Further, the analysis demonstrates that incorporation of an additional single RH-stable external additive (e.g., the hydrophobic silica used in Fig. 13) can destabilize an otherwise RH-stable toner/carrier pair, if the stability of the latter is based on a parallel toner/RH and carrier/RH response. Additionally, for developers based on multiple external additives, the analysis (by extension) suggests that RH-stability may be achieved if various opposing responses can be balanced. Finally, the analysis reinforces the view that particular RH-stable developer designs involve specific responses and are thus not universally applicable—stability achieved by a matching or balancing of individual RH-responses may be lost if even a single component of the developer is altered.

Clearly, RH-stable developers based on multiple additives potentially involve a large number of interactive factors—Eq.37 expanded to include an RH-response for each term would be impressively complex! As a result, progress in this area requires careful execution of well-designed experiments—as should be evident from the above discussions on additive effects and RH effects, measurements taken at a single "standard" mixing time can be particularly misleading. It is also important to note that RH-stability "design rules" based solely on experimental observations may lack general applicability—an "RH-stable" design optimized for styrene/ acrylate-based toners or steel carriers may be totally ineffective for polyester-based toners or ferrite carriers.

5. Concluding Remarks

In this review, developer stability has been discussed only in terms of the average toner *q/m* value. However, for robust xerographic performance, there are many other important factors—e.g., developer conductivity, toner flow, etc. Also, while image development is broadly controlled by the *q/m* value of a toner, the distribution of charge is an additional important metric for overall development. For example, the stability of a xerographic system with respect to background development will be affected by the "low charge/ wrong-sign" population in the distributed spectrum of toner charge, and this unwanted population can be generated by slow toner/carrier charge exchange, etc. Since these additional factors can also exhibit "aging" or unstable behavior, it is clear that the design of a truly stable developer is a task of unlimited potential complexity.

Another important area not discussed in this review is the impact of materials processing on developer performance. Toner melt-mix conditions can strongly affect the distribution of toner components,[11,13] and thereby affect toner performance, and the mode and degree of external additive blending can affect toner properties such as flow, charge level and admix rate.[18,41-44] Thus, even for a fixed toner recipe, there can be variability in *q/m* performance, as a result of processing differences .

While the examples cited in this review are all based on two-component development, many of the modes of instability will be of equal relevance to single-component development. Indeed, while elegantly simple in concept, single component development offers only limited opportunities for feedback process control, and this limitation therefor imposes critical stability requirements with respect to toner charge and other factors such as flow, adhesion, etc.

Finally, the evident success of a wide range of commercial toner/developer designs indicates that the challenges of stability can be met via a variety of strategies, and that creative materials inventors can yet prevail in an area of technology where the underlying physics and chemistry are still imperfectly understood.

6. Acknowledgements

As long-time colleagues, Dr. J. T. Bickmore and Dr. E. J. Gutman have provided a continual supply of challenging experimental data and theoretical insights. Our career-long study of toner/developer properties has also been facilitated by a succession of technical managers who have encouraged a scientific approach to studies in an area of applied development.

7. References

1. L. B. Schein, Chapters 6 and 7, *Electrophotography and Development Physics*, Springer, New York, 1988.
2. U. S. Patent, 5,225,872.
3. U. S. Patent. 5,237,369.

4. U. S. Patent, 4,314,755.
5. U. S. Patent, 5,183,964.
6. E. J. Gutman and G. C. Hartmann, *J. Imaging Sci. and Technol.*, 36 (4), 335-349, (1992).
7. J. H. Anderson, *J. Imaging Technol.*, 16 (6), 204-208, (1990).
8. U. S . Patent, 4,590,141.
9. R. J. Nash and J. T. Bickmore, *4th Int'l. Cong. on Adv. in Non-Impact Printing Technol.*, A. Jaffe, ed., SPSE, Springfield, VA, 113-126 (1988).
10. S. C. Hart, J. J. Folkins and C. G. Edmunds, *6th Int'l. Cong. on Adv. in Non-Impact Printing Technol.* R. J. Nash, ed., IS&T, Springfield, VA, 44-54, (1990).
11. J. H. Anderson, D. E. Bugner, L. P. DeMejo, R. A. Guistina and N. Zumbulyadis, *8th Int'l. Cong. on Adv. in Non-Impact Printing Technol.*, E. Hanson, ed., IS&T, Springfield, VA, 107-115, (1992) .
12. J. Guay, J. L. Miller, H. Nguyen and A. F. Diaz, *8th Int'l. Congress on Adv. in Non-Impact Printing Technol.*, E. Hanson, ed., IS&T, Springfield, VA, 116-118, (1992).
13. J. H. Anderson, D. E. Bugner and R. A. Guistina, *8th Int'l. Cong. on Adv. in Non-Impact Printing Technol.*, E. Hanson, ed., IS&T, Springfield, VA, 144-149, (1992).
14. A. R. Gutierrez, D. Fenzel-Alexander, D. Mc.Kean and A. F. Diaz, *8th Intl. Cong. on Adv. in Non-Impact Printing Technol.*, E. Hanson, ed., IS&T, Springfield, VA, 163-166, (1992).
15. R. J. Nash and J. T. Bickmore, *9th Int'l. Cong. on Adv. in Non-Impact Printing Technol.*, M. Yokohama, ed., IS&T, Springfield, VA, 68-71, (1993) .
16. A. Stuebbe, *7th. Int'l. Cong. on Adv. in Non-Impact Printing Technol.*, K. Pietrowski, ed., IS&T, Springfield, VA, 240-249, (1991).
17. A. R. Guitierrez, H. T. Nguyen and A. F. Diaz, *8th Int'l. Cong. on Adv. in Non-Impact Printing Technol.*, E. Hanson, ed., IS&T, Springfield, VA, 122-125, (1992).
18. U. S. Patent, 5,296,324.
19. U. S. Patent, 5,272,040.
20. U. S. Patent, 5,066,558.
21. U. S. Patent, 4,555,467.
22. U. S. Patent, 4,623,605.
23. U. S. Patent, 5,120,631.
24. U. S. Patent, 5,024,915.
25. U. S. Patent, 4,513,074.
26. U. S. Patent, 5,139,914.
27. U. S. Patent, 4,960,664.
28. U. S. Patent, 3,983,045.
29. R. J. Nash, *5th. Int'l. Cong. on Adv. in Non-Impact Printing Technol.*, J. S. Moore, ed., SPSE, Springfield, VA, 158-165,(1989).
30. U. S . Patent, 4,920,023.
31. U. S Patent, 5,171,653.
32. U. S. Patent, 4,585,723.
33. U. S. Patent, 4,618,556.
34. U. S. Patent, 5,176,979.
35. U. S. Patent, 5,178,984.
36. U. S. Patent, 5,215,848.
37. U. S. Patent, 5,256,511.
38. U. S. Patent, 4,027,621.
39. U. S. Patent, 4,495,267.
40. L. B. Schein, Chapter 4, *Electrophotography and Development Physics*, Springer, New York, 1988.
41. U. S. Patent, 5,147,753.
42. U. S. Patent, 5,178,460.
43. U. S. Patent, 5,202,213.
44. U. S. Patent, 5,307,127.